AAPS PharmSciTech (2023) 24:20
https://doi.org/10.1208/s12249-022-02479-3

RESEARCH ARTICLE

Advancements in Amorphous Solid Dispersions to Improve Bioavailability

Self-Assembled Lipid Polymer Hybrid Nanoparticles Using Combinational Drugs for Migraine Via Intranasal Route

Preeti Dali[1] · **Pravin Shende**[1]

Received: 10 October 2022 / Accepted: 29 November 2022 / Published online: 16 December 2022

Abstract

The objective of the current research study was to formulate the PEGylated lipid polymer hybrid nanoparticles of ergotamine and caffeine for intranasal administration with higher entrapment efficiency, better permeability, desirable controlled release pattern, and significant brain uptake in animal studies. A single-step nanoprecipitation method was employed in the processing of self-assembled hybrid nanoparticles constituting polymer PLGA, lipids soya lecithin, and DPPC with PEGylation using polyethylene glycol (PEG-2000). The optimal lipid/polymer weight ratio of 15% w/w showed lower particle size of 239.46 ± 2.31 nm with good colloidal stability depicted by zeta potential (− 18.36 ± 6.59 mV), higher entrapment efficiency of 86.88 ± 1.67%, and controlled release profile when evaluated for *in vitro* and *ex vivo* studies as 97.12 ± 2.79% and 75.13 ± 5.62% release, respectively, for 48 h. The formulation showed long-term serum stability when incubated in bovine serum albumin and displayed high brain uptake (4.35-fold) offering significant permeability in the brain post-intranasal administration via olfactory route. Histopathological investigations and serotonin toxicity studies in animals confirmed the safe and non-toxic nature of the formulation while the acetic acid writhing test proved the anti-hyperalgesic activity. The PEGylated lipid polymer hybrid nanoparticles of ergotamine and caffeine showed synergistic activity with efficacious higher anti-migraine potential.

Highlights

- PEGylated lipid polymer hybrid nanoparticles exhibit a core–shell assembly with higher loading efficiency, biocompatibility, and enhanced steric stability.
- Hybrid nanoparticles using combination of drugs illustrated long-term serum stability.
- Ergotamine hybrid nanoparticles demonstrated higher uptake and sustained presence in brain.

Keywords ergotamine · hybrid nanoparticles · lipid/polymer weight ratio · nanoprecipitation · serotonin syndrome · serum stability

Abbreviations

ERT	Ergotamine tartrate
CFN	Caffeine
HNPs	Hybrid nanoparticles
PEG	Polyethylene glycol
CNS	Central nervous system
5-HT	5-Hydroxy tryptamine
CMC	Critical micelle concentration
RES	Reticuloendothelial system
BSA	Bovine serum albumin
Tm	Melting transition temperature
PXRD	Powdered X-ray diffraction
ATR-FTIR	Attenuated total reflection-Fourier transform infrared
DSC	Differential scanning colorimetry
NMR	Nuclear magnetic resonance
SEM	Scanning electron microscopy
IAEC	Institutional Animal Ethics Committee
PVDF	Polyvinyl diflouride
BCS	Biopharmaceutical Classification System

✉ Pravin Shende
shendepravin94@gmail.com

[1] Shobhaben Pratapbhai Patel School of Pharmacy and Technology Management, SVKM's NMIMS, Vile Parle (W), Mumbai, India

Introduction

Nanotechnology employs nano-dimensional structures to deliver chemical agents ranging from small size actives, proteins, and genes to diagnostic agents [1, 2]. Among various

nanoparticulate formulations, two classes of nano-system like polymer-based and lipid-based nanostructures are investigated. Each class of these nanoparticulate structures possesses advantages like steric stabilization, higher payloads, and biocompatibility, whereas disadvantages like drug leakage and low entrapment. Lipid nanoparticles display drawbacks like absence of structural integrity resulting in drug leakage and poor storage stability while polymeric nanoparticles demonstrate low encapsulation and inadequate release of drugs with plasma fluctuations [3, 4]. To overcome such limitations, a novel class of delivery vehicle emerged as lipid polymer hybrid nanoparticles (HNPs) that exhibit the complementary characteristics of physical stability and biocompatibility [5, 6]. The HNP structure constitutes three functional components in the form of an inner core of polymer containing therapeutic drug (BCS class II and IV) with high payload, surrounded by a layer of lipids around the core of polymer that offers biocompatibility and augments drug retention within the polymer core. Moreover, the third layer of lipid-PEG enhances stability and prolongs *in vivo* circulation time by steric stabilization [7–9]. The polymer core and surrounding lipid layers are linked via van der Waals forces of attraction or hydrophobic interactions, whereas the water-soluble polymer core is coupled via covalent bonds with the surrounding lipids in hybrid nanoparticles [10, 11]. Most HNPs are synthesized by the single-step method that comprises simple mixing of aqueous dispersion of lipids with organic solution of polymer using the nanoprecipitation method to exhibit cost-effectiveness and scalability [12, 13].

In HNPs, the lipid/polymer (L/P) weight ratio is important such that an optimum L/P weight ratio of 15% w/w is required to adequately coat the polymer core uniformly and offer monodisperse nanoparticles [14]. Higher L/P weight ratio resulted in higher lipid concentration than critical micelle concentration (CMC) leading to the formation of liposomes of lipids other than HNPs, whereas lower L/P weight ratio leads to HNP aggregation because of incomplete lipid coating [15]. Valencia *et al*. demonstrated the ideal ratio of 1:10 for lipid:PLGA by varying the amounts of lipids and polymer PLGA from 1:1, 1:10, to 1:1000 with the measurements of zeta potential and particle size of hybrid nanoparticles using microfluidics rapid mixing for nanoprecipitation of the polymer [16]. The optimal ratio of 1:10 for lipid to polymer provided homogenous and stable nanoparticles with adequate lipid coverage and the molecular weight of PLGA and the end-group of lipids determined the charge on particles [17]. Based on the prior literature and studies, this research work focused on optimizing the L/P weight ratio in a range of 10 to 25% w/w with characterization of nanoparticles using anti-migraine compound ergotamine tartrate (ERT) and caffeine (CFN) selected as the solubilizer and permeation enhancer for ERT [18, 19]. For migraine treatment, ERT is considered the first choice owing to its structural similarity to many neurotransmitters like dopamine, serotonin, and 5-hydroxy tryptamine. ERT exhibited instability to heat, light, and moisture, and its marketed formulations with caffeine as a CNS stimulant, such as film-coated tablets, orally disintegrating tablets and suppositories, showed poor bioavailability. Hence, the present work focused mainly on stabilization of the active (ERT) by nanoencapsulation technique to improve its stability and further use of intranasal route to enhance its absorption in brain via olfactory route by bypassing the blood–brain barrier. Use of biomimetic lipids like lecithin and DPPC form spherical-shaped nanoparticles due to their self-assembling characteristics. The polymer of choice was PLGA because of its biodegradable nature and FDA-approval status for medical applications. Further, PEGylation of nanoparticles assist to improve the *in vivo* circulation time by imparting stealth properties [20, 21]. The current research work aimed to design a PEGylated lipid polymer hybrid nanoparticles using PLGA polymer, lecithin, and DPPC lipids and PEGylation performed using polyethylene glycol (PEG-2000) for higher entrapment efficiency, good permeability, and controlled release rate of ERT with long-term serum stability and higher brain uptake. The research work also aimed to prove safe and non-toxic nature of hybrid nanoparticles for intranasal use by conducting serotonin toxicity studies and histopathological evaluation.

Materials and Methods

Materials

Resomer® RG 503 H (poly-acid terminated, lactide: glycolide 50:50, M_W: 24,000–38,000) was procured from Evonik, USA. Lipoid S 100 (phosphatidylcholine from soyabean) was obtained from Lipoid, Germany. Ergotamine tartrate (ERT) was purchased from Teva Czech Industries, Czech Republic. CFN was received as gift sample from Aarti drugs, Mumbai, India. Polyethylene glycol (PEG-2000, M_W: 1900–2200) was obtained from Merck (USA). Water purified from MilliQ® Integral Water Purification System was used for preparation and analysis. Analytical reagent grade chemicals were used throughout the experiments.

Methods

Self-assembled HNPs for ERT were prepared using single-step nanoprecipitation technique [4], wherein Resomer and ERT were dissolved in acetone under magnetic stirring to form a clear solution. Aqueous lipid dispersion phase consisting of DPPC and soya lecithin in a ratio of 2:1 with the hydrophilic drug CFN dispersed in water which was heated at 65–70°C, above the Tm (melting phase transition temperature) of lipids to form milky uniform dispersion. The organic polymer phase was added to aqueous lipid dispersion phase drop-wise under homogenization

(Homogenizer, Remi, India) resulted into polymer nanoprecipitation and self-assembly of lipids around the polymeric core linked via hydrophobic interactions. The solvents were then removed from the nanosuspension by stirring it at ambient temperature for 2 h. The nanoparticles were then given stealth properties after addition of 1 mL PEG-2000 solution (10% v/v) to the nanosuspension by probe sonication with a 30% amplitude pulse ON/OFF for 15 s and subjected to such three cycles. Lipid hydrophobic tails were attached to the ERT-containing polymer core of PLGA, and hydrophilic heads with CFN were bonded to the surrounding environment to produce HNPs with steric stabilization by PEG-2000. Using solvent evaporation, the HNPs were then further centrifuged at 2000 rpm (Remi, India) for 15 min to remove extra lipids and polymer [22]. The particle size and PDI of hybrid nanoparticles depended on polymer PLGA concentration, mixing speed during addition of polymer and lipid, and solvent-volume ratio. The final nanosuspension was lyophilized in a freeze drier (Labconco, USA) for 24 h and abbreviated as HNP. The blank formulation was prepared using the same method of preparation without drugs and abbreviated as HNP-PL.

Experimentation

The experiments were conducted to optimize the lipid/polymer weight ratio to achieve the stable and homogenous hybrid nanoparticles and their characterization is shown in Table I. The polymer PLGA concentration varied while lipid concentration was kept constant to get the various L/P weight ratios and the impact of ratio evaluated based on the characteristics of HNPs.

Characterization of Optimized Hybrid Nanoparticles

Zeta Potential Measurements, Particle Size Analysis, and Polydispersity Index

The prepared HNPs were characterized for particle size by employing Malvern Zetasizer, UK, which operates on a dynamic light scattering approach. Surface zeta potential is the electrokinetic potential on the surface of hybrid nanoparticles measured using the Malvern Zetasizer [23]. Adequate dilutions of the formulations HNP-01, HNP-02, and HNP-03 were performed using double distilled water (MilliQ, France) and measurements were taken in triplicate.

Table I Formulation Chart of HNPs

S. no	Formulation code	L/P weight ratio	Polymer PLGA concentration (mg)	Level of PLGA
1	HNP-01	10%	30	+1
2	HNP-02	15%	20	0
3	HNP-03	25%	10	-1

Drug Entrapment Efficiency (% EE)

In the % EE measurements, the lyophilized hybrid nanoparticles HNP-01, HNP-02, and HNP-03 were weighed as 33.53 mg of solids which is equivalent to 1 mg of ERT and 30 mg of CFN, mixed with 10 mL with phosphate buffer pH 6. This aqueous dispersion was filtered and the supernatant was evaluated for free drug using UV–visible spectrophotometer (PerkinElmer, USA). The aqueous dispersions of HNP formulations were centrifuged (Remi, India) at 8000 rpm for 30 min at 25°C, and the supernatant solution was filtered through a Nylon membrane filter (Millipore, USA). The filtrate was examined by UV–visible spectrophotometer at the wavelengths of 240 and 273 nm for ERT and CFN, respectively. % EE was calculated using the following formula:

$$\%\ \mathrm{EE} = \left(\frac{\text{Quantity of drug encapsulated in hybrid nanoparticles}}{\text{Total quantity of drug added}}\right) \times 100$$

In Vitro Release Studies

In vitro release studies for ERT and CFN were conducted by means of Franz diffusion cell using dialysis membrane (Mw: 10,000–12,000, Himedia Labs, India) in phosphate buffer pH 6 with temperature maintained at 37°C ± 0.5°C. Formulations (HNP-01, HNP-02, and HNP-03) were weighed accurately and dispersions prepared in 3 mL of phosphate buffer pH 6. Since the HNP formulations developed using biodegradable and controlled-release polymer PLGA, the *in vitro* release study was performed for an extended period of 48 h. Sample aliquots were withdrawn as per the protocol at scheduled timepoints of 0.5,1,2, 3, 4, 6, 24, and 48 h and studied using UV–visible spectrophotometer (Perkin Elmer, USA) at the wavelengths of 240 nm for ERT and 273 nm for CFN.

In Vitro Stability in Serum

The stability of serum in nanoparticles is a fundamental aspect of drug delivery *in vivo* as most of the polymer-based and lipid-based nanoparticles showed drug leakages due to significant membrane permeability [24]. To evaluate the drug leakages in serum, HNP formulations were incubated in a solution of 1 mg/mL of 10% bovine serum albumin (BSA), kept at 37°C with gentle magnetic stirring. Aliquots of HNP solutions were withdrawn at predefined intervals to measure particle size and PDI by Malvern Zetasizer Nano-ZS 90, UK. A polymer-based nanoparticle formulation prepared constituting PLGA

polymer for comparison with HNPs incubated in 10% BSA solution for 8 h to evaluate any change in particle size.

Based on the above characterization, the optimized formulation of hybrid nanoparticles HNP-02 was selected for evaluation of *ex vivo* release, attenuated total reflection-Fourier transform infrared (ATR-FTIR), differential scanning colorimetry (DSC), XRD, ^{1}H nuclear magnetic resonance (NMR), SEM, and *in vivo* and stability studies.

Ex Vivo Release Study

The *ex vivo* drug release studies were performed on goat nasal mucosa procured from a nearby slaughterhouse located in Vile Parle, Mumbai, India. The nasal mucosa was carefully taken from the animal after it was slaughtered, cleaned, and submerged in a cold phosphate-buffered solution pH 6 for 2 h. Serosal surface of the mucosal membrane faced the recipient chamber while the mucosal surface was positioned between the donor and receiver chambers of the Franz diffusion cell device. The receiver chamber was filled with 20 mL of phosphate buffer 6, which was then swirled slowly at 300 rpm while maintaining the temperature at 37° ± 0.5°C. The formulation HNP-02 was accurately weighed and examined for *ex vivo* study with aliquots withdrawn at pre-defined timepoints of 0.5, 1, 2, 3, 4, 6, 24, and 48 h. Further analysis was conducted utilizing UV–visible spectrophotometer (Perkin Elmer, USA) at the wavelengths of 240 nm for ERT and 273 nm for CFN.

Attenuated Total Reflection-Fourier Transform Infrared Spectroscopy

The infrared spectra of ERT, CFN, blank HNP-PL and formulation HNP-02 were examined using ATR-FTIR spectrophotometer (Perkin Elmer, USA) with wavelength ranging from 500 to 4000 cm^{-1} and resolution of 4 cm^{-1}.

Differential Scanning Colorimetry

Accurately weighed samples of ERT, CFN, and formulation HNP-02 were evaluated employing DSC (Mettler Toledo, DSCI/500, Switzerland) at the temperature ranging from 50 to 350°C with a 10°C/min scanning rate under an inert nitrogen atmosphere.

Powdered X-ray Diffraction Studies

The crystallinity of pure drugs ERT and CFN was studied with optimized formulation HNP-02 using Rigaku SmartLab Powder X-ray diffractometer (Rigaku Corporation, Japan). The samples were analyzed in triplicate by irradiating with CuK α radiation at 45 kV, 2 theta angle range of 0°–90°, and a scanning rate of 3°/min.

^{1}H Nuclear Magnetic Resonance

The ^{1}H NMR spectra estimate nuclear spin in samples using 60-MHz NMR spectrometer (Spinsolve-60 carbon, Magritek, Germany). Samples of ERT, CFN, blank HNP-PL, and hybrid nanoparticles HNP-02 were measured using deuterated DMSO.

Morphological Analysis

Scanning electron microscopy was used to evaluate the surface morphology of the hybrid nanoparticle HNP-02 and the blank HNP-PL (SEM, Zeiss, Germany). The surface morphology of the test samples was analyzed using a narrow beam of electrons after mounting on the aluminum stubs using adhesive tapes which were previously coated with platinum alloy under vacuum.

Animal Studies

Pharmacokinetics Study Animal studies were conducted on Sprague–Dawley male rats weighing 200 ± 30 g in compliance with the approved protocol from Institutional Animal Ethics Committee (IAEC) with protocol number of CPCSEA/DIPS/150322/25. Prior to initiation of pharmacokinetics study, the animals were fasted for 18 h and allowed free access to food and water with the utmost care taken during studies to avoid any discomfort to animals [25]. For study, the animals were divided into 3 groups ($n = 3$) with pure drug ERT as standard group, control (normal saline), and test formulation HNP-02 administered via an intranasal route with the help of micropipette. Post-administration of formulation, the brain tissues were collected from each group for the estimation of drug content using HPLC method. Animals were sacrificed at selected timepoints by cervical dislocation and brains were carefully dissected out. The dissected brain further rinsed with sufficient volume of normal saline, homogenized using polytron homogenizer (Kinematica AG, Switzerland), and precipitated using methanol as a diluent. These diluted methanolic samples were centrifuged at 7000 rpm, 15 min for removal of any suspended debris, and subjected to analysis with HPLC parameters as BDS Hypersil C8 column, and mobile phase (formic acid: methanol, 30:70) with a column flow rate of 1.0 mL per min and UV detector at a wavelength of 240 nm.

Pharmacodynamics Study The pharmacodynamics study was conducted employing the acetic acid writhing test that induces hyperalgesia, the most significant symptom of migraine in serotonin-controlled animals. Male Wistar rats weighing between 180 and 220 g were housed in ventilated cage system with five animals in each group. Three groups were formed wherein the first group of animals was

administered the test sample HNP-02 intranasally equivalent to 1 mg of ERT, the second group administered pure drug abbreviated as ERT treated, and normal saline administered to the third group denoted as control. All three groups were later injected with acetic acid injection of 0.3% w/v via intraperitoneal route. The acetic acid injection acts as an irritant generating pain in animals mimicking pain as in migraine. Anti-hyperalgesic activity was determined as the count of abdominal constrictions observed during the 15-min interval post-acetic acid injection 0.3% w/v.

Histopathology Evaluation of Brain Tissues The brain tissue was carefully removed after pharmacokinetics studies and immersed in formalin solution for 2 h. Hematoxylin and eosin were used to stain the samples and then examined using an optical microscope (AX80, Olympus, Tokyo, Japan). The tissues were observed for any abnormalities like presence of inflammation, degeneration, necrosis, or hemolysis [26].

Serotonin Toxicity Studies

Serotonin toxicity is a potentially life-threatening condition observed due to higher serotonin levels in the body that result in to change in mental status, autonomic hyperactivity, and neuromuscular abnormalities. Overstimulation of post-synaptic 5-HT1A and 5-HT1B receptors leads to an increase in serotonin levels caused by a certain class of drugs like serotonin reuptake inhibitors (fluoxetine, sertraline, venlafaxine, duloxetine), MAO inhibitors (phenelzine, selegiline), and anti-depressants (clomipramine, imipramine, nortriptyline) which show more adverse effects as compared to other drugs like anti-migraine compounds (ergot alkaloids and triptans) [27, 28]. Hence, this study was performed on HNP-02 to assess the impact of formulation on serotonergic activity in animals in compliance with the approved protocol from the IAEC (Protocol number: CPCSEA/DIPS/150522/26). The male Wistar rats weighing 190–210 g were segregated into three groups ($n=5$) drug-treated, i.e., ERT-treated group, formulation HNP-treated group, and control group. Post 1 h of intranasal administration of samples, different neuromuscular excitations were monitored which represent the serotonergic syndrome response. Using nominal scale approach for evaluation of serotonin syndrome, the scores were determined based on the presence or absence of response.

Stability Testing

According to ICH guidelines "Q1A (R2) 2003, Stability Testing of New Drug Substances and Products," formulation HNP-02 was monitored for accelerated stability testing [29]. Samples of formulation HNP-02 were stored at 25°C ± 2°C/65% ± 5% RH and refrigerated at 4°C ± 1°C for 3 months in the glass vials. Samples were monitored at 1, 2, and 3 months wherein lyophilized hybrid nanoparticles were dispersed using MilliQ water with nanoparticulate suspensions sonicated for 10–15 s and examined for particle size, ZP, % entrapment efficiency, and % *in vitro* release studies.

Statistical Analysis

The statistical assessment employed to analyzed parameters using GraphPad prism 5 software (California, USA) with results expressed as mean ± SD. One-way ANOVA followed by Dunnett's multiple comparison test was used to evaluate the data from pharmacodynamics investigations and differences were deemed as statistically significant at ***p 0.001 and highly significant at ****p 0.0001.

Results

Zeta Potential Measurements, Particle Size Analysis, and PDI

Particle size uniformity is controlled by factors such polymer amount, solvent-volume ratio, and stirring speed, which influenced the ZP, particle size, and PDI of hybrid nanoparticles.

The data in Table II indicated the importance of optimal balance between particle size and surface charge of nanoparticles and its homogeneity in distribution within the colloidal system. The particle size for pure drug ERT was observed to be 684.2 ± 13.48 nm, whereas the formulation HNPs showed lower particle size ranging from 239.46 ± 2.31 to 484.28 ± 14.25 nm across the various L/P weight ratios. The polymer PLGA (Resomer 503H) with acid end-group showed

Table II ZP, Particle Size, and PDI Measurements

S. no	Formulation	Formulation code	ZP (mV ± SD)	Particle size (nm ± SD)	PDI (n ± SD)
1	Ergotamine tartrate	ERT	− 21.65 ± 7.89	684.2 ± 13.48	0.572 ± 0.18
2	Resomer (30 mg)	HNP-01	− 8.95 ± 6.42	373.23 ± 7.32	0.687 ± 0.33
3	Resomer (20 mg)	HNP-02	− 18.36 ± 6.59	239.46 ± 2.31	0.196 ± 0.24
4	Resomer (10 mg)	HNP-03	− 9.03 ± 3.92	484.28 ± 14.25	0.396 ± 0.37

negative zeta values for all experiments. Formulation HNP-01 showed higher PDI (0.687 ± 0.33) and lower zeta potential (− 8.95 ± 6.42 mV) attributed to the incomplete coverage by lipids due to low lipid content and higher polymer content (30 mg). The nanoparticles with higher polymer content generally showed lower particle size at initial stage and later tend to aggregate over the period of time due to the partial surface coverage by the lipids indicated by higher polydispersity index (0.687 ± 0.33). Formulation HNP-03 showed higher particle size of 484.28 ± 14.25 nm and lower ZP of − 9.03 ± 3.92 mV (similar to HNP-01) attributed to higher lipid concentration than polymer that resulted in extra layer of lipids covering the particle surface and formation of separate lipid liposomes leading to larger particle size and polydispersity index (0.396 ± 0.37). However, formulation HNP-02 showed low particle size (239.46 ± 2.31 nm) with PDI of 0.196 ± 0.24 (less than 0.3) indicated homogeneity, whereas high ZP (− 18.36 ± 6.59 mV) demonstrated good colloidal stability attributed to complete coverage of polymer surface by the lipids that inhibit aggregation of particles for prolonged time. Hence, the particle size and ZP data revealed the ideal L/P weight ratio of 15% w/w to be an important parameter which was further confirmed by conducting *in vitro* stability study for the HNPs in 10% BSA (Bovine serum albumin).

Drug Entrapment Efficiency (% EE)

Drug entrapment efficiency conducted for HNP-01, HNP-02, and HNP-03 showed higher entrapment for HNP-02 as shown in Fig. 1. The order of % EE observed to be HNP-02 > HNP-01 > HNP-03 confirmed that the L/P weight ratio of 15% w/w was optimum. ERT and polymer PLGA were readily solubilized in organic solvent like acetone and further surrounded by lipid coating (lecithin and DPPC) resulted in improved solubility of ERT both in polymer PLGA and in lipids due to its lipophilic nature that attributed to the higher entrapment efficiency for formulation HNP-02. This also demonstrated the complete covering of lipids on polymer core that increased the entrapment of ERT to 86.88 ± 1.67% as compared with other formulations that displayed 67.26 ± 2.83% and 46.71 ± 2.41% for HNP-01 and HNP-03, respectively. Lower polymer content (10 mg) and higher lipid content (100 mg) in HNP-03 that exceeded critical micelle concentration of lipids affect the encapsulation process resulting in lower entrapment of drug (46.71 ± 2.41%). Similarly, the higher entrapment for CFN was observed in formulation HNP-02 of 37.09 ± 0.68% as compared to other formulations with values of 30.12 ± 0.44% and 28.81 ± 0.72% for HNP-01 and HNP-03, respectively. Lower entrapment efficiency of CFN attributed to hydrophilic nature of the molecule. Further, during preparation of HNPs, CFN was dissolved in aqueous dispersion of lipids and heated above the melting transition temperature, Tm of lipid (DPPC), that resulted in partial dissolution of CFN.

In Vitro Release Study (%)

Figure 2 illustrated the *in vitro* release study carried out for formulations HNP-01, HNP-02, and HNP-03 at an extended period for 48 h. The controlled release patterns for both ERT and CFN observed were in order of

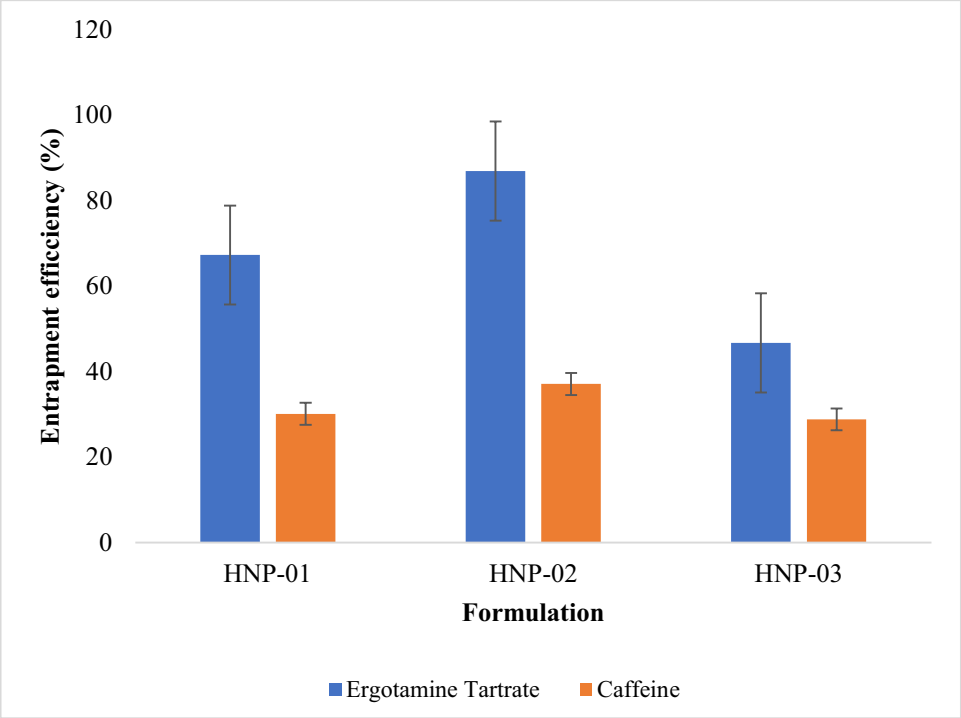

Fig. 1 % EE for formulations HNP-01, HNP-02, and HNP-03

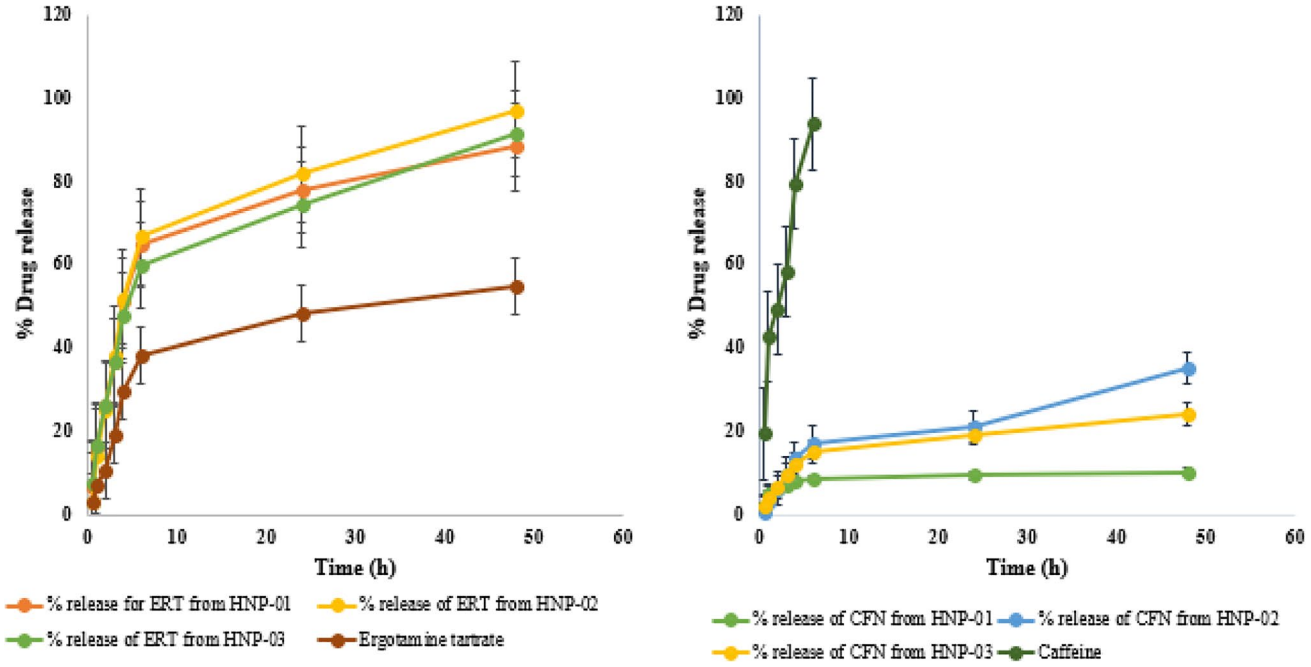

Fig. 2 % *In vitro* release for ERT and CFN from formulations HNP-01, HNP-02, and HNP-03

HNP-02 > HNP-03 > HNP-01. The formulation HNP-02 showed higher release profile for ERT to be 97.12 ± 2.79% at 48 h, followed by HNP-03 that demonstrated drug release of 91.42 ± 1.46% and 88.31 ± 1.95% for HNP-01 as compared to the incomplete release of 54.76 ± 2.26% for plain ERT within 48 h. A similar pattern was observed for CFN with significant release of 35.26 ± 2.53% from HNP-02 followed by HNP-03 with release of 24.14 ± 1.83% and lowest release of 10.37 ± 0.76% from HNP-01 in comparison to plain CFN with premature release of 93.71 ± 8.17% within 6 h. The controlled release pattern of drugs from HNPs was attributed to the compact PLGA matrix surrounded by lipid coating that resisted the process of diffusion by restricting the flow of release medium with slow release of the contents. The outcome of *in vitro* release studies was consistent with that of results of entrapment efficiency.

In Vitro Stability in Serum

Figure 3a and b illustrated the *in vitro* serum stability for formulation HNP-02 and polymer nanoparticles (NPs) made of PLGA incubated in 10% BSA solution. The data of particle size and PDI measured for formulation HNP-02 showed no significant difference as shown in Fig. 3a which confirmed the stability of HNP-02 in serum. The formulation HNP-02 depicted retention in particle size over a range of 239.4 ± 2.31–425.6 ± 8.96 nm when studied for 8 h and PDI varied in a narrow range from 0.196 ± 0.24 to 0.459 ± 0.78 and hence proved its stability in serum for prolonged period of 8 h.

The above data of particle size, ZP, %EE, *in vitro* release profile, and *in vitro* stability in serum confirmed HNP-02 to be the optimized formulation and hence selected for additional evaluation of *ex vivo* release, FTIR, DSC, XRD, NMR, SEM, *in vivo* studies, and stability testing.

Figure 3b shows the highest retention in particle size for HNP-02 (239.4 ± 2.31–425.6 ± 8.96 nm) as compared to the other HNP formulations when studied for 24 h. HNP-03 showed higher particle size (484.2 ± 14.25–610.4 ± 9.32 nm) due to the formation of excess lipid liposomes and HNP-01 that showed increase in particle size (373.2 ± 7.32–965.3 ± 11.53 nm) for a period of 24 h that confirmed higher polymer concentration and incomplete coverage of lipids with low particle size initially but tend to aggregate later due particle coalescence. However, the polymer nanoparticles (NPs) showed a dramatic increase in particle size from 331.3 ± 8.67 to 1284.2 ± 22.63 nm within a short period of 3 h after incubation in 10% BSA solution. Thus, HNP-02 exhibited long-term serum stability (24 h) due to complete coverage of lipids over the polymer core and the lipid-PEG outermost coating prevented the adsorption of proteins on surface of the nanoparticles with higher circulation time *in vivo*.

Ex Vivo Release Study

Figure 4 illustrated the *ex vivo* release profile of ERT and CFN for the optimized formulation HNP-02. The

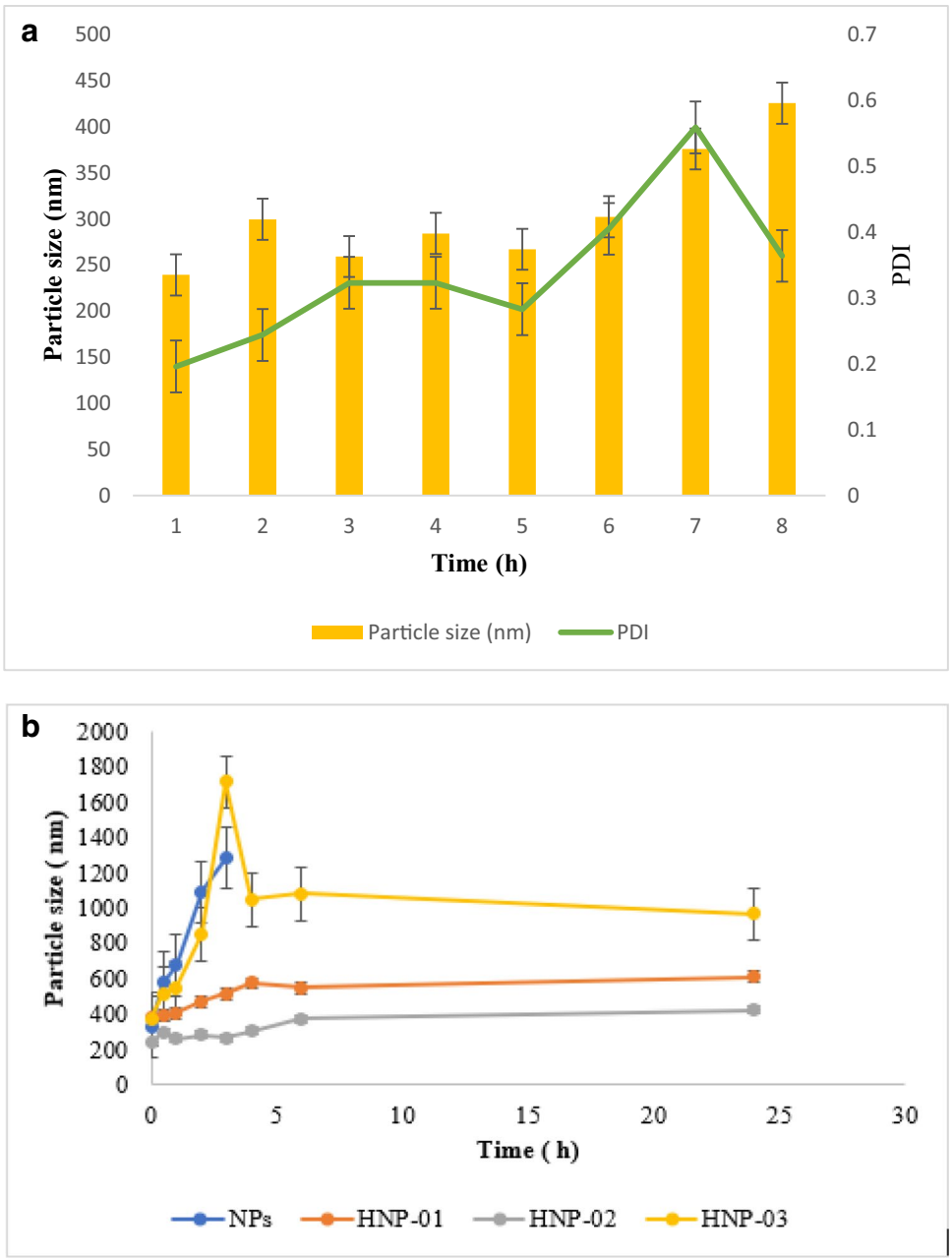

Fig. 3 **a** *In vitro* stability in bovine serum albumin for formulation HNP-02. **b** Particle size (nm) in 10% BSA solution for NPs and formulations HNP-01, HNP-02, and HNP-03

observed values of *ex vivo* release for ERT and CFN were 75.13 ± 5.62% and 23.03 ± 1.38%, respectively, against the *in vitro* profile of 97.12 ± 2.79% and 35.26 ± 2.53% for ERT and CFN, respectively, that revealed the controlled release pattern for HNPs. This confirmed the core–shell structure for HNPs because the shell of lipids over the polymer core prevented the interaction with the external physiological environment and also the optimum L/P weight ratio that led to complete coverage of lipids on to the polymer core to restrict the entry of surrounding biological medium in to the HNPs [30].

FTIR Spectroscopy

The FTIR spectra of ERT, CFN, soya lecithin, DPPC, PLGA, and formulation HNP-02 are shown in Fig. 5. Plain ERT spectrum showed characteristic peaks ranging from 3200 to 3334 cm^{-1} corresponding to hydroxyl and amine groups, whereas peaks for carbonyl stretch were observed in the region of 1646 to 1723 cm^{-1}. FTIR spectrum of CFN showed two characteristic peaks, one for amide group in the range of 2800 to 3120 cm^{-1} and second for carbonyl stretch in the region of 1552 to 1784 cm^{-1}. The

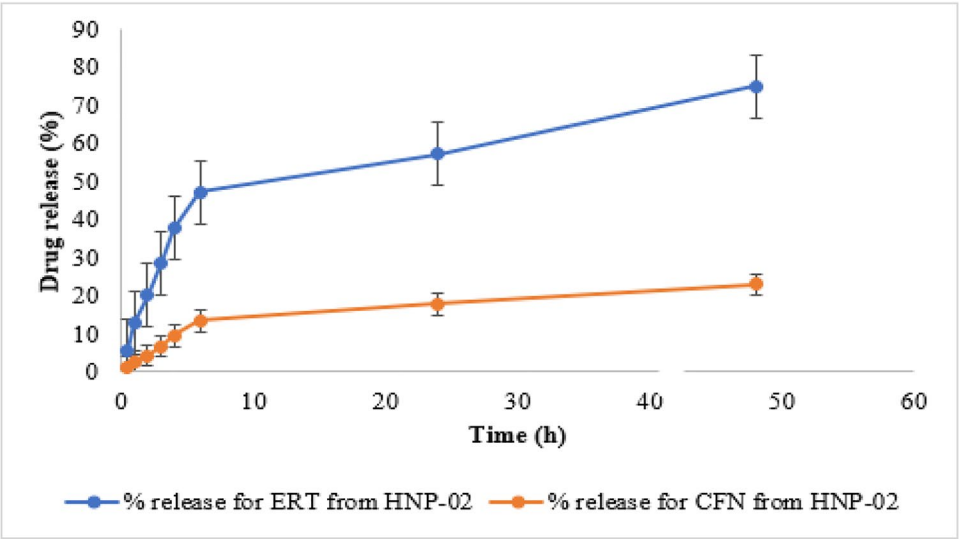

Fig. 4 *Ex vivo* drug release for ERT and CFN from formulation HNP-02

characteristic bands for DPPC observed were at 2912 cm^{-1} (C–H stretching), 1732 cm^{-1} (carbonyl symmetric stretching), 1377 cm^{-1} (C–H bending), and 1054 cm^{-1} (P–O–C stretching), respectively. Lecithin showed characteristic bands in the region of 3376 cm^{-1} for N–H stretch, 3010 cm^{-1} for *cis*-double bond stretching, 1735 cm^{-1} for carbonyl (C = O stretch), and 1083 cm^{-1} for P–O–C stretching. The IR spectrum of PLGA showed carbonyl stretching at 1753 cm^{-1} and 1382 cm^{-1} as C–H bending whereas 1087–1170 cm^{-1} for C–O stretching. The formulation HNP-02 spectrum matched with DPPC absorption bands but showed a slight shift of characteristic bands at 2925 cm^{-1} for N–H stretch, 1712 cm^{-1} for carbonyl stretch, and 967 cm^{-1} for O–H bending in drug-loaded hybrid nanoparticles, and disappearance of the characteristic peaks of ERT and CFN indicated encapsulation of drugs in self-assembled lipid-polymer matrix by van der Waals forces and hydrophobic interactions [31].

DSC Studies

DSC thermograms of ERT, CFN, and formulation HNP-02 are depicted in Fig. 6. The thermogram for ERT showed two melting endotherms: one at 86°C as water of crystallization and the second was the degradation at 214°C. The drug CFN displayed a sharp melting endotherm for degradation at 236°C. The DSC thermogram for the formulation HNP-02 exhibited no such peaks and the only endotherm seen in the range of 52–55°C might be assigned to lecithin (Tm = 47.2°C), polymer PLGA (melting point = 50°C), and PEG 2000 that collectively showed melting endotherm at 53°C. Peak diminishments in HNP-02 indicated the entrapment of ERT and CFN in the core–shell structure of hybrid nanoparticles and the conversion of crystalline state into an amorphous form. This conversion to amorphous form led to solubility enhancement and complete entrapment of drugs in the hybrid nanoparticles with improved thermal stability [32, 33].

Powdered X-ray Diffraction Studies

Figure 7 illustrates the X-ray diffractograms of ERT, CFN, and formulation HNP-02, wherein XRD for ERT showed characteristic peaks at 2 theta values of 12°, 13°, 16°, 19°, 21°, and 26° denoting the crystalline nature and similar XRD pattern for CFN showed crystalline peaks at 2 theta values of 10°, 25°, 26°, and 27°. The disappearance of peaks for ERT and CFN in diffractogram of lyophilized formulation HNP-02 indicated the loss in crystallinity because of lyophilization and entrapment in hybrid nanoparticles seen due to self-assembly of lipid-polymer network with conversion to amorphous state. These results were in agreement with DSC studies and expected to increase the solubility of drugs [34].

^{1}H NMR Spectroscopy

Figure 8 illustrates the proton NMR spectra for ERT, CFN, blank HNP-PL, and formulation HNP-02. The spectrum of ERT showed aliphatic methoxy protons at 3.5–4.3 ppm and CFN showed peaks of N-methyl protons at 3.33, 3.5, and 3.94 ppm. The spectrum for blank HNP-PL showed protons resonating at 1.5 ppm corresponding to protons of polylactic acid and the resonance seen in region of 4.5–5.1 ppm due to methyl protons of polyglycolic acid part of PLGA. The resonance seen in the region of 3.0–3.5 ppm depicted DPPC methyl protons in HNP-PL. The spectrum of HNP-02 showed peak diminishments

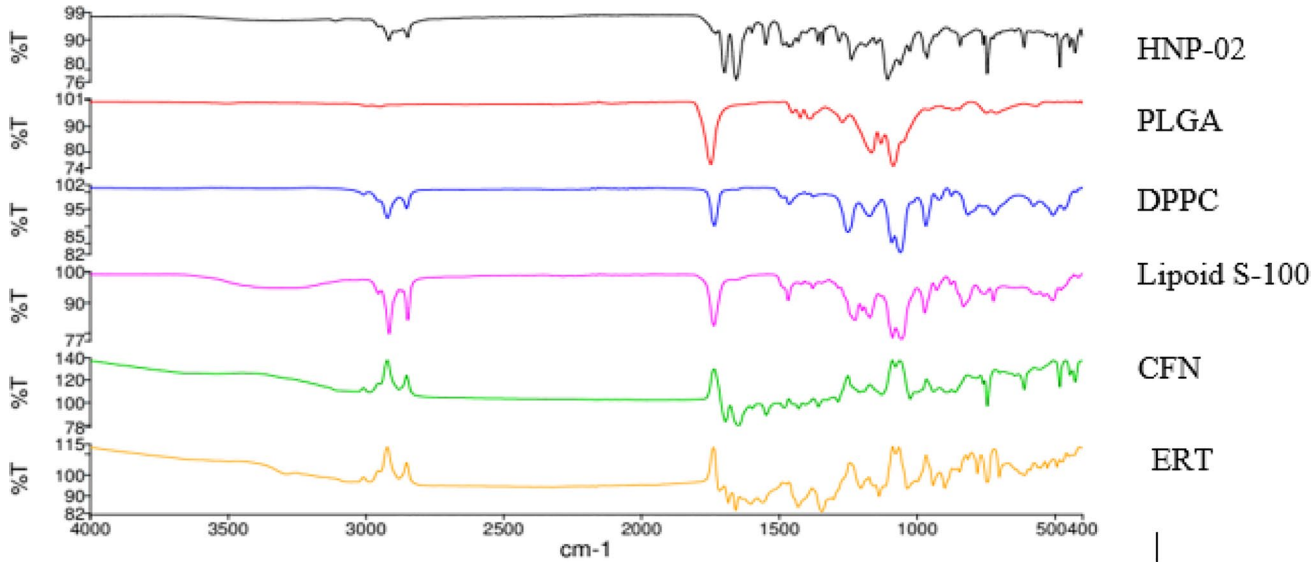

Fig. 5 FTIR spectra for ERT, CFN, Lipoid S-100, DPPC, PLGA, and formulation HNP-02

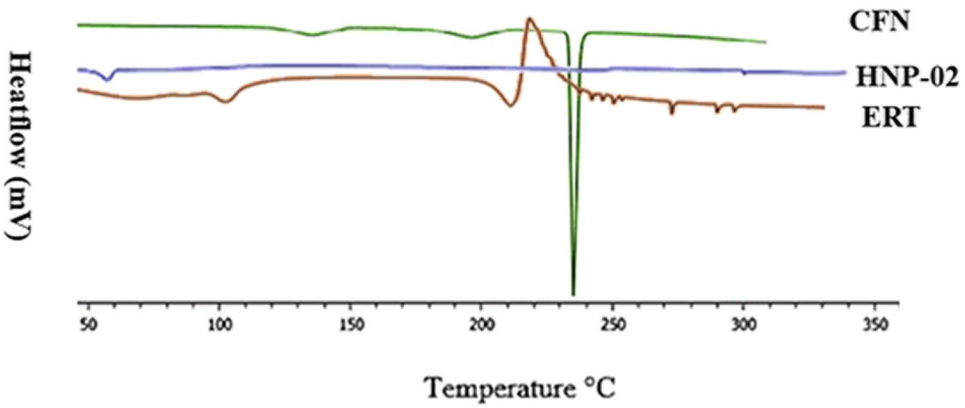

Fig. 6 DSC thermograms of ERT, CFN, and formulation HNP-02

that indicated low mobility due to entrapment in the core–shell assembly of polymer and lipids. The slow orientation of protons attached to hybrid nanoparticles showed no interaction between the protons because the protons were packed in an ordered manner in the bilayer membrane, and the only identified protons were of the methyl and methylene groups resonating between 3.3 and 4.5 ppm which correspond to trimethyl ammonium group located in the hydrophilic part of the bilayer of lipids. However, the formulation HNP-02 showed diminishment of peaks for ERT, CFN, and blank HNP-PL that confirmed the complete entrapment of drugs ERT and CFN in the core–shell structure of polymer and lipids with no significant interaction between drugs and other ingredients used in the formulation [35].

Morphological Analysis

The morphological analysis was conducted using SEM that revealed spherical homogenous nanoparticles with a rough surface as shown in Fig. 9a, wherein roughness was attributed to lyophilization of nanoparticles. Figure 9b depicts a two-layer structure for hybrid nanoparticles with PLGA core and lipid coating observed as the boundary that exhibited onion-like morphology with multilamellar stacks of lipids surrounding the polymeric core [36, 37].

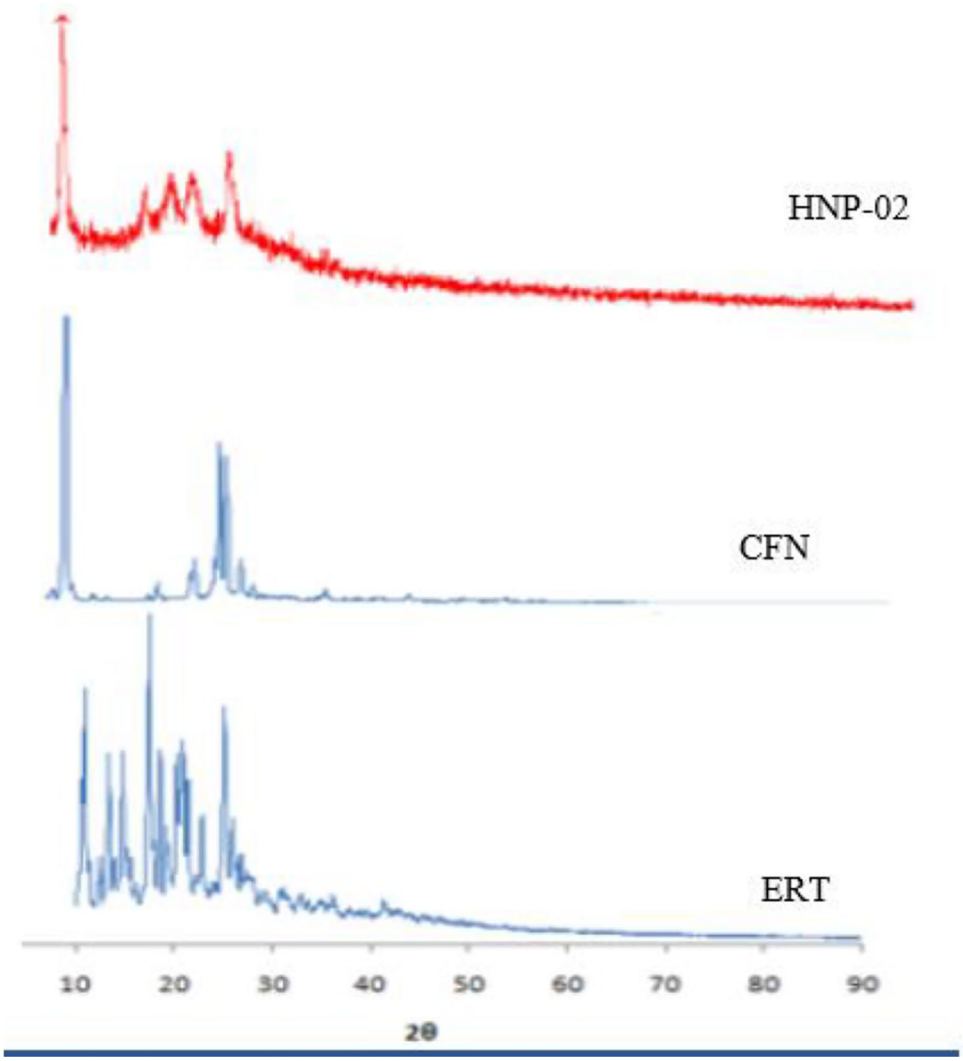

Fig. 7 XRD diffractograms of ERT, CFN, and formulation HNP-02

Animal Studies

Pharmacokinetics Study

The drug concentration in the brain was assessed at predefined intervals of 30, 60, and 90 min by an *in vivo* study using a validated HPLC method. The data for ERT alone and in comparison, with test sample HNP-02, are illustrated in Fig. 10. The data for ERT showed an increase in brain uptake from 1.2 (30 min) to 3.45 ng/mL (60 min) with a decline to the initial level of 1.32 ng/mL at 90 min. The results illustrated that C max for ERT reached within 60 min and then the concentration declined rapidly within 90 min which matched with the prior literature studies of ERT. However, the formulation HNP showed a steep rise in drug concentration from 1.48 ng/mL at 30 min to 4.68 ng/mL at 60 min and further increased to 5.74 ng/mL until 90 min. Hence, it was concluded that the hybrid nanoparticles exhibited higher absorption in the brain and a further rise in concentration depicted the accumulation in the brain due to the nano size and entrapment in biodegradable polymer PLGA and the biomimetic lipids [38]. In comparison to ERT intranasal administration, HNP-02 demonstrated a 4.35-fold increase in brain uptake with accumulation in brain for longer period of 90 min. These results verified that the core–shell structure of lipid polymer hybrid nanoparticles not only shielded the drug ERT from the external physiological environment but also enhanced its absorption through the olfactory pathway for nose-to-brain delivery. Moreover, the outermost lipid-PEG layer prevented the reticuloendothelial uptake that illustrated the potential of HNP-02 to successfully enter the brain by avoiding the blood–brain barrier and effectively treat the migraine.

Pharmacodynamics Study

The pharmacodynamics study was conducted on male Wistar rats using intraperitoneal injection of acetic acid

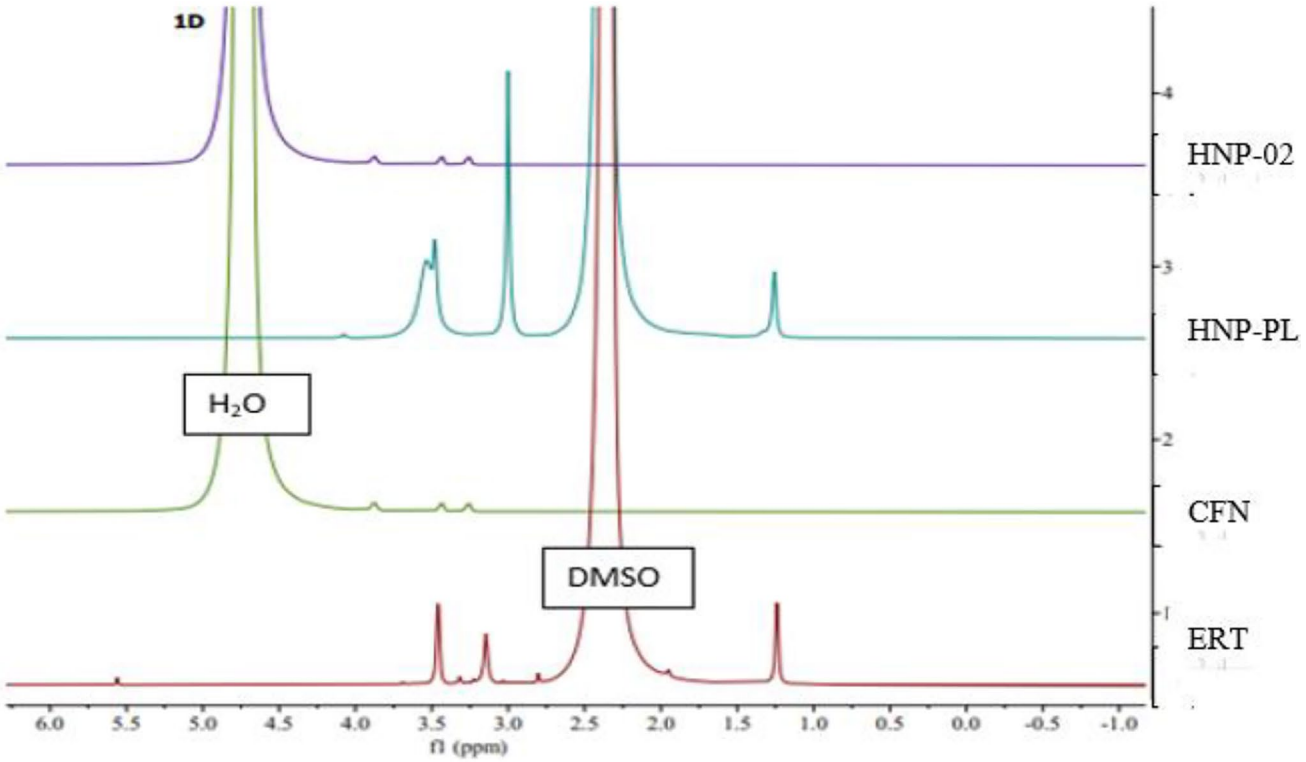

Fig. 8 ^{1}H NMR spectra for ERT, CFN, blank HNP-PL, and formulation HNP-02

0.3% w/v. This injection used as an irritant in animals and resulted in abdominal constrictions with stretching of hind limbs and generated pain similar to that arose during migraine attack. The test sample HNP-02 along with ERT and control samples were administered intranasally using normal saline as a vehicle with subsequent administration of acetic acid injection intraperitoneally. The number of abdominal constrictions counted for 15 min post-acetic acid injection in all animals ($n=5$). Figure 11 depicts the scores for samples tested wherein the control sample scored 34.1, whereas ERT-treated group showed 24.6 number of abdominal constrictions with the lowest value of 17.3 for HNP-treated group. Statistical evaluation proved highly significant difference for HNP-treated group (****$p<0.0001$) as compared to control group, whereas ERT-treated group showed statistically significant difference (***$p<0.001$) against the control. It was evident from the PD results that formulation HNP-02 after intranasal administration showed a significantly reduced number of abdominal constrictions by exhibiting anti-hyperalgesic activity in the treatment of migraine when compared with the plain drug.

Histopathology Investigation

Figure 12 illustrates the microscopic observations for brain tissue of 3 groups: control, ERT-treated, and HNP-treated

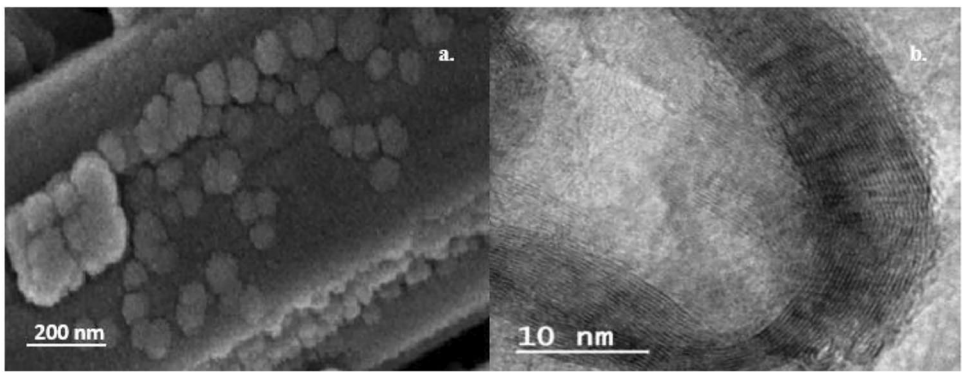

Fig. 9 SEM images for **a** hybrid nanoparticles (HNP-02) and **b** core–shell structure

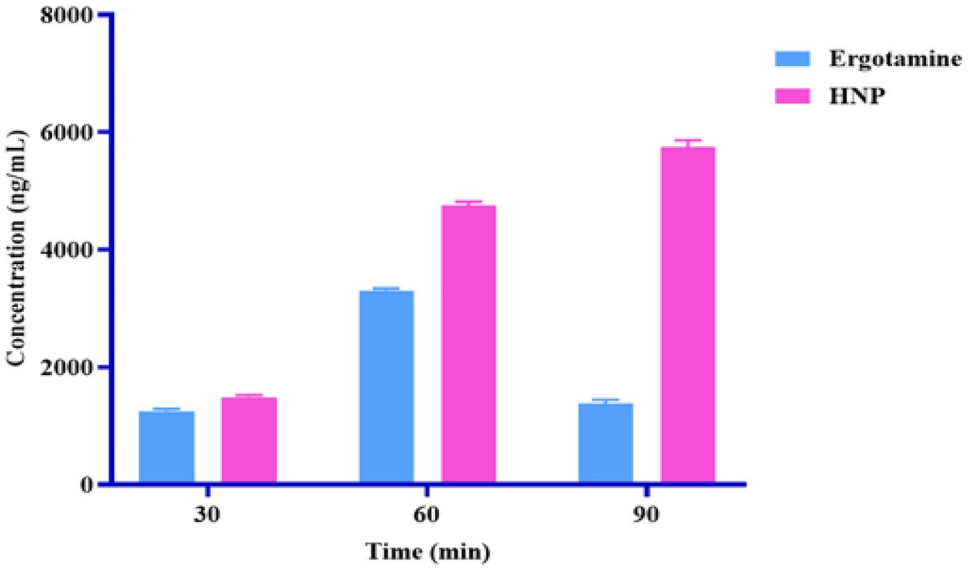

Fig. 10 ERG concentration in brain at intervals of 30, 60, and 90 min

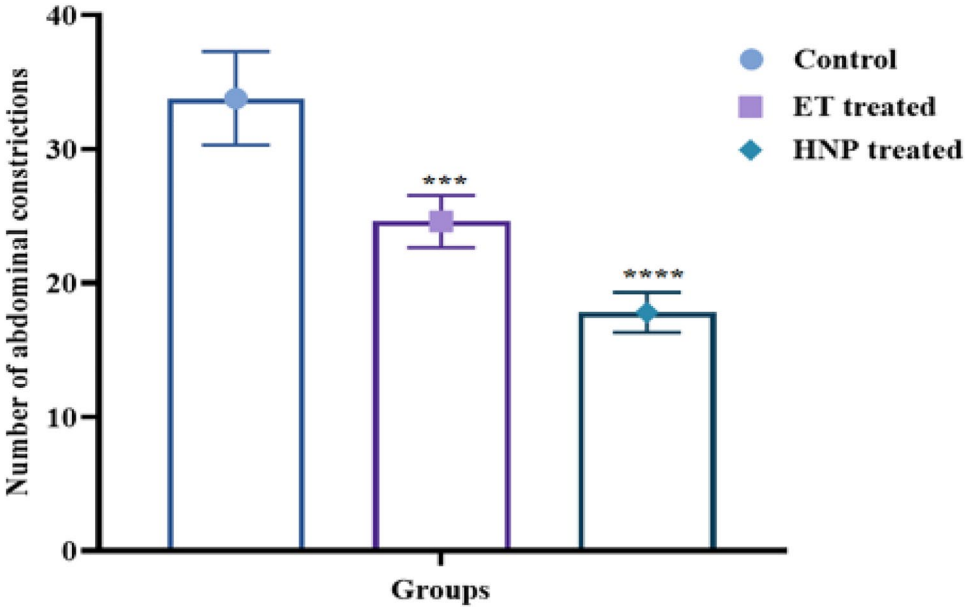

Fig. 11 Acetic acid induced writhing test in control, ERT-treated, and HNP-treated groups. Values are expressed as mean ± SD ($n = 5$). One-way ANOVA followed by Dunnett's multiple comparison test revealed ****$p < 0.0001$ highly significant difference for HNP-treated group compared with control when administered intranasally and ***$p < 0.001$ considered statistically significant for ERT-treated vs control

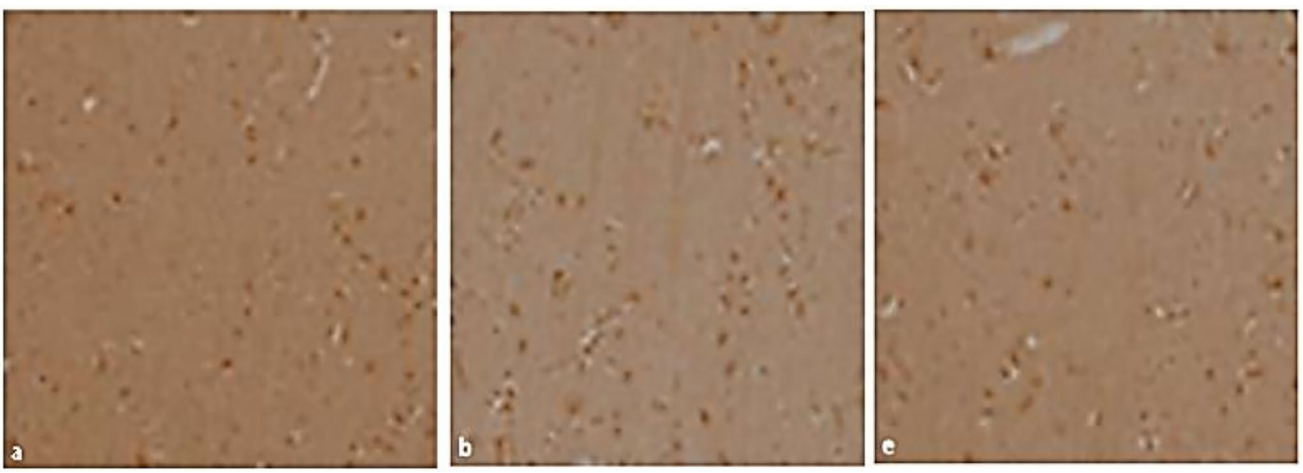

Fig. 12 Histopathological images: **a** control, **b** ERT-treated, and **c** HNP-treated groups

groups. The histopathological investigations revealed normal nucleated cells with no abnormalities as compared to control, in both ERT-treated and HNP-treated groups. The glial cells were seen of normal size and morphology without signs of inflammation or haemolysis and absence of macrophage infiltration, which thus confirmed that formulation HNP-02 was safe and non-toxic for intranasal administration [39, 40].

Serotonin Toxicity Studies

Excess serotonin levels in the body led to neuromuscular contractions, autonomic hyperactivity, and mental status changes. Hence, serotonin syndrome was studied for drugs that increase the concentration of serotonin in the body. Animals were divided into three groups, i.e., untreated, ERT-treated, and HNP-treated, wherein various behavioral responses were studied in animals with scores calculated post 1 h nasal administration as mentioned in Table III. The symptoms like neuromuscular excitations generate responses like head twitches, tremors, hind limb abduction, straub tail, head shaking, head weaving, flat low body posture, and backward walking, whereas autonomic dysregulation symptoms show responses of hyperactivity and hyperreactivity while other symptoms of hallucinations and bowel sounds show responses of pilo erection and defaecation [41]. These responses were assessed using a nominal scale approach viz. categorical response represented as presence or absence of symptoms and the overall scores calculated.

Table III data revealed the score card for three groups, viz., untreated, ERT-treated, and HNP-treated groups, wherein the untreated group showed complete absence of responses to the neuromuscular symptoms with score denoted as zero. The ERT-treated group showed a score of 10 out of 12 responses that reported the presence of symptoms, whereas the HNP-treated group depicted a score of 5 out of 12 responses. The score denoted based on response received from 1 or 2 animals out of the total 5 animals tested for the presence of symptoms which was termed to be a mild response on the scale of mild-moderate-severe. Hence, it was concluded that no severe response was observed for any of the symptoms evaluated for the HNP-treated group and thus HNP formulation showed no serotonin toxicity and termed to be efficacious in the treatment of migraine.

Table III Serotonin Response Score Card

Behavioral response 1 h post-administration	Untreated	ERT-treated	HNP-treated
Head twitches	0	1	1
Tremors	0	1	0
Hind limb abduction	0	2	1
Straub tail	0	0	0
Head shaking	0	1	0
Head weaving	0	1	0
Flat low body posture	0	1	0
Backward walking	0	0	0
Hyperactivity	0	2	2
Hyperreactivity	0	2	2
Pilo erection	0	2	1
Defecation	0	1	0

Stability Studies

During accelerated stability performed on HNPs, characteristics like particle size measurements, ZP, % entrapment efficiency, and % *in vitro* release studies were investigated, and the stability results are illustrated in Table IV. The HNP samples as lyophilized cakes were dispersed in distilled water and the aqueous dispersions were analyzed. During stability testing at refrigerated and room temperature conditions, no significant change was observed in any of the studied parameters. The results were well within the limits $\pm$ 5% of the average value complying with the stability criteria. This confirmed the stability of lyophilized HNP at specified conditions.

Discussion

Using nanoprecipitation method, the formulation HNP-02 with an ideal L/P weight ratio of 15% w/w showed low particle size and PDI with good colloidal stability. The % entrapment efficiency was higher for HNP-02 due to the lipophilic nature of ERT and also during preparation, ERT was dissolved in PLGA and solvents that improved the solubility along with self-assembling of lipids led to significant entrapment efficiency. Similar results were observed by Mohammad and co-workers for tacrolimus-loaded core–shell lipid-polymer hybrid nanoparticles which revealed higher entrapment with optimum L/P weight ratio and higher particle size with increased concentration of polymer (30% w/w) [42]. The impact of polymer concentration on the release profile for both ERT and CFN was evident from the *in vitro* and *ex vivo* release data which indicated the controlled release pattern because of the formation of a compact polymer matrix of PLGA surrounded by lipid coating to restrict the entry of release medium. Also, higher PLGA content (25% w/w) showed an optimistic effect on the particle size of HNPs which resulted in higher particle size with low surface area and controlled release rate pattern. Incubation in 10% BSA solution showed particle size retention for 24 h that exhibited long-term serum stability for HNPs, and this was confirmed by results of formulation

Table IV Stability Results for HNP-02

Stability condition	PS (nm ± SD)	ZP (mV ± SD)	EE (% ± SD)	*In vitro* release (% ± SD)
Initial	**239.4 ± 0.28**	**− 18.36 ± 6.59**	**86.88 ± 1.67**	**97.12 ± 2.79**
1 M/4°C	251.42 ± 1.32	− 19.32 ± 7.82	87.16 ± 1.34	95.26 ± 3.91
1 M/25°C	282.91 ± 1.01	− 17.77 ± 5.17	85.23 ± 2.65	93.81 ± 4.62
3 M/4°C	271.55 ± 2.68	− 21.21 ± 4.94	84.29 ± 2.39	94.17 ± 3.87
3 M/25°C	382.68 ± 3.19	− 16.33 ± 9.25	85.72 ± 4.18	96.73 ± 6.48

Bold entries indicated the optimized formulation

HNP-02. Similar findings were confirmed by Pengju Ma and his coworkers for bupivacaine-loaded lipid-polymer hybrid nanoparticles that exhibited controlled release pattern owing to core shell structure and improved *in vitro* stability of hybrid nanoparticles in 10% v/v fetal bovine serum (FBS) when compared against bupivacaine-loaded PLGA nanoparticles (NPs) in order to simulate the *in vivo* hemocompatibility [24]. The lipid-PEG outermost coating of HNP formulation displayed an insignificant impact in serum because of the existence of PEG-2000 which prevented the adsorption of proteins on the surface of nanoparticles and increased *in vivo* circulation time. Thus, the outer PEG layer exhibited two functions, first the maintenance of *in vitro* stability of HNPs by reducing the nanoparticle aggregation and second evading the recognition by the reticuloendothelial system (RES) and other immune cells *in vivo*.

The FTIR study for HNP-02 matched with the characteristic bands of DPPC and indicated entrapment of actives in the core–shell structure of hybrid nanoparticles due to van der Waals forces of attraction or hydrophobic interactions. DSC study demonstrated diminishments in the characteristic peaks of ERT and CFN and confirmed the entrapment of actives in the lipid-polymer network. These results were in line with earlier findings of methotrexate-loaded lipid-polymer hybrid nanoparticles for controlled drug delivery applications that demonstrated conversion of crystalline to amorphous form or disorganized crystal lattice of drug during entrapment in hybrid nanoparticle [32]. Absence of crystalline peaks was attributed to strong interactions with lipids during fabrication of lipid-polymer hybrid nanoparticles. Powdered X-ray diffraction studies revealed the loss of crystallinity and conversion to amorphous form by increasing the solubility of the actives in hybrid nanoparticles. ^{1}H NMR spectra illustrated the disappearance of characteristic peaks of actives and low mobility of protons as they were packed in the orderly configuration in the bilayer membrane of lipids. This confirmed no interaction between actives and excipients employed in the formulation with the entrapment of actives in the strong lipid-polymer network. Morphological evaluation by SEM represented homogenous spherical nanoparticles, and the multilayered stacks of lipids around the polymer core depicted the onion-like structure confirmed the lipid coverage around the polymer core. Similar morphology of onion-like structure was observed around the PLGA core by Bershteyn *et al*., in a DOPC-based hybrid nanoparticles [43].

Pharmacokinetics studies for HNP-02 confirmed the higher brain concentration (4.35-fold rise) post-intranasal administration. The nano-size of HNPs and entrapment in biodegradable polymer PLGA surrounded with biomimetic lipids helped to traverse the nanoparticles via the olfactory pathway and bypassed the blood–brain barrier (BBB) reaching the brain. The rise in brain concentration of formulation HNP-02 and its accumulation in the brain for the time interval of 90 min studied was found to be much higher as compared to ERT alone proving the efficacy of formulation HNP-02 in the treatment of migraine. The results from pharmacodynamics study proved the reduction of hyperalgesic effect with formulation HNP-02 indicated by the lowest number of abdominal constrictions counted after the intraperitoneal administration of acetic acid injection 0.3% w/v that induced pain similar to migraine in the animals. Histopathological evaluation confirmed no change in glial cells depicting absence of abnormality and necrosis or inflammation. Histopathology studies of nasal mucosa conducted by Galgatte and his coworkers for sumatriptan succinate mucoadhesive gel confirmed absence of cell necrosis or removal of epithelium of nasal mucosa [44]. The serotonin toxicity score card revealed low scores for formulation HNP-02 confirmed by the mild response for neuromuscular excitations and mental changes observed post-intranasal administration depicted by the absence of serotonergic syndrome in animals. Zhiyuan *et al*. conducted similar serotonin-toxicity syndrome elicited by 5-hydroxy-L-tryptophan in clorgyline-pretreated rats and studied the behavioral relationship associated with serotonin toxicity and the receptors mediating these behavioral changes [45]. Accelerated stability testing conducted for 3 months showed no significant impact on any of the parameters tested and complied with the stability specification criteria. Hence, it was concluded that the formulation HNP-02 was found to be stable, safe, non-toxic in nature with higher brain uptake and reduction in hyperalgesia without serotonin toxicity after intranasal administration to confirm HNP formulation reached the brain via olfactory route.

Conclusion

The outcome of the current study illustrated that PEGylated hybrid nanoparticles can be prepared using the nanoprecipitation method with L/P weight ratio (15% w/w) with lower particle size (239.46 ± 2.31 nm), higher zeta potential (− 18.36 ± 6.59 mV), and higher entrapment efficiency (86.88 ± 1.67%). Controlled release pattern for both drugs ERT and CFN proved by *in vitro* and *ex vivo* testing. In the presence of biological enzymes and serum, the investigations revealed the lipids self-assembled around the PLGA core to form a core–shell structure that displayed long-term stability to hybrid nanoparticles against particle aggregation. The *in vivo* results showed greater brain uptake (4.35-fold) and demonstrated anti-hyperalgesic activity with reduction in pain showed by acetic acid writhing test. Overall, the results confirmed that optimized hybrid nanoparticles with the L/P weight ratio 15% w/w demonstrated higher entrapment, and controlled delivery along with long-term stability in serum. The increased brain absorption without serotonin toxicity supported the therapeutic effectiveness of HNP in treatment of migraine when administered intranasally.

Funding No grants received from funding agencies in the public, commercial, or not-for-profit sectors for this research work.

Declarations

Credit Statement Preeti Dali: paper writing, experimentation.

Dr. Pravin Shende: conceptualization, research planning.

Conflict of Interest The authors declare no competing interests.

References

1. Dave V, Tak K, Sohgaura A, Gupta A, Sadhu V, Reddy KR. Lipid-polymer hybrid nanoparticles: synthesis strategies and biomedical applications. J Microbiol Methods. 2019;160:130–42. https://doi.org/10.1016/j.mimet.2019.03.017.
2. Ferreira Soares DC, Domingues SC, Viana DB, Tebaldi ML. Polymer-hybrid nanoparticles: current advances in biomedical applications. Biomed Pharmacotherapy. 2020;131:110695. https://doi.org/10.1016/j.biopha.2020.110695.
3. Mohanty A, Uthaman S, Park IK. Utilization of polymer-lipid hybrid nanoparticles for targeted anti-cancer therapy. Molecules. 2020;25(19):4377. https://doi.org/10.3390/molecules25194377. (**Published 2020 Sep 23.**).
4. Raman S, Mahmood S, Rahman A. A review on lipid- polymer hybrid nanoparticles and preparation with recent update. Mater Sci Forum. 2020;981:322–7.
5. Vikulina AS, Skirtach AG, Volodkin DV. Hybrids of polymer multilayers, lipids, and nanoparticles Mimicking the cellular microenvironment. Langmuir. 2019;35(26):8565–73.
6. Leng D, et al. Engineering of budesonide-loaded lipid-polymer hybrid nanoparticles using a quality-by-design approach. Int J Pharm. 2018;548(2):740–6.
7. Chan Juliana M, Zhang Liangfang, Yuet Kai P, Liao Grace, Rhee June-Wha, Langer Robert, Farokhzad Omid C. PLGA–lecithin–PEG core–shell nanoparticles for controlled drug delivery. Biomaterials. 2009;30(8):1627–34. https://doi.org/10.1016/j.biomaterials.2008.12.013.
8. Thevenot Julie, Troutier Anne-Lise, David Laurent, Delair Thierry, Ladavière Catherine. Steric stabilization of lipid/polymer particle assemblies by poly (ethylene glycol)-lipids. Biomacromolecules. 2007;8(11):3651–60. https://doi.org/10.1021/bm700753q.
9. Tahir N, Haseeb MT, Madni A, Parveen F, Khan MM, Khan S, Jan N, Khan A. Lipid polymer hybrid nanoparticles: a novel approach for drug delivery. In: Tyagi, RK, Garg N, Shukla R, Bisen PS editors. Role of Novel Drug Delivery Vehicles in Nanobiomedicine [Internet]. London: IntechOpen; 2019 [cited 2022 Nov 01]. Available from: https://www.intechopen.com/chapters/69735. https://doi.org/10.5772/intechopen.88269
10. Mortar G. Hybrid Lipid-polymer nanoparticulate delivery, The invention relates to a nanoparticulate colloidal delivery vehicle comprising a biodegradable polymer. 2007;1–17.
11. Liu Yutao, Pan Jie, Feng Si-Shen. Nanoparticles of lipid monolayer shell and biodegradable polymer core for controlled release of paclitaxel: effects of surfactants on particles size, characteristics and in vitro performance. Int J Pharm. 2010;395(1–2):243–50. https://doi.org/10.1016/j.ijpharm.2010.05.008. (**ISSN 0378-5173**).
12. Moon J James, et al. Antigen-displaying lipid-enveloped PLGA nanoparticles as delivery agents for a Plasmodium vivax malaria vaccine. PloS one. 2012;7.2:e31472.
13. Mieszawska AJ, Gianella A, Cormode DP, Zhao Y, Meijerink A, Langer R, et al. Engineering of lipid-coated PLGA nanoparticles with a tunable payload of diagnostically active nanocrystals for medical imaging. Chem Commun. 2012;48:5835–7. https://doi.org/10.1039/C2CC32149A.
14. Zhang L, Chan JM, Gu FX, Rhee J-W, Wang AZ, Radovic-Moreno AF, Alexis F, Langer R, Farokhzad OC. Self-assembled lipid polymer hybrid nanoparticles: a robust drug delivery platform. ACS Nano. 2008;2:1696–702.
15. Ali S, Amin MU, Tariq I, Sohail MF, Ali MY, Preis E, et al. Lipoparticles for synergistic chemo-photodynamic therapy to ovarian carcinoma cells: in vitro and in vivo assessments. Int J Nanomedicine. 2021;16:951–76.
16. Valencia PM, Basto PA, Zhang L, Rhee M, Langer R, Farokhzad OC, Karnik R. Single-step assembly of homogenous lipid-polymeric and lipid-quantum dot nanoparticles enabled by microfluidic rapid mixing. ACS Nano. 2010Mar 23;4(3):1671–9. https://doi.org/10.1021/nn901433u.
17. Hadinoto K, Sundaresan A, Cheow WS. Lipid-polymer hybrid nanoparticles as a new generation therapeutic delivery platform: a review. Eur J Pharm Biopharm. 2013;85(3 Pt A):427–43. https://doi.org/10.1016/j.ejpb.2013.07.002.
18. Arnold AC, Ramirez CE, Choi L, Okamoto LE, Gamboa A, Diedrich A, et al. Combination ergotamine and caffeine improves seated blood pressure and pre-syncopal symptoms in autonomic failure. Front Physiol. 2014;5:1–7.
19 Dali P, Shende P. Inclusion complex of cyclodextrin with ergotamine and evaluation of cyclodextrin-based nanosponges. J Incl Phenom Macrocycl Chem. 2020;102:S45–S1. https://doi.org/10.1007/s10847-022-01149-y.
20. Nag OK, Awasthi V. Surface engineering of liposomes for stealth behavior. Pharmaceutics. 2013;5:542–69. https://doi.org/10.3390/pharmaceutics5040542.
21. Ling Guixia, Zhang Peng, Zhang Wenping, Sun Jin, Meng Xiaoxue, Qin Yimeng, Deng Yihui, He Zhonggui. Development of novel self-assembled DS-PLGA hybrid nanoparticles for improving oral bioavailability of vincristine sulfate by P-gp

inhibition. J Control Release. 2010;148(2):241–8. https://doi.org/10.1016/j.jconrel.2010.08.010. (**ISSN 0168-3659**).
22. Suk JS, Xu Q, Kim N, Hanes J, Ensign LM. PEGylation as a strategy for improving nanoparticle-based drug and gene delivery. Adv Drug Deliv Rev. 2016;99:28–51. https://doi.org/10.1016/j.addr.2015.09.012.
23. García-González CA, et al. Production of hybrid lipid-based particles loaded with inorganic nanoparticles and active compounds for prolonged topical release. Int J Pharm. 2009;382(1–2):296–304.
24. Ma P, Li T, Xing H, et al. Local anesthetic effects of bupivacaine loaded lipid-polymer hybrid nanoparticles: in vitro and in vivo evaluation. Biomed Pharmacother. 2017;89:689–95. https://doi.org/10.1016/j.biopha.2017.01.175.
25. Wang Y, Yang X, Yang J, Wang Y, Chen R, Jing Wu, Liu Y, Zhang N. Self-assembled nanoparticles of methotrexate conjugated O-carboxymethyl chitosan: preparation, characterization and drug release behavior in vitro. Carbohyd Polym. 2011;86(4):1665–70.
26. Masjedi M, Azadi A, Heidari R, Mohammadi-Samani S. Nose-to-brain delivery of sumatriptan-loaded nanostructured lipid carriers: preparation, optimization, characterization and pharmacokinetic evaluation. J Pharm Pharmacol. 2020;72(10):1341–51. https://doi.org/10.1111/jphp.13316.
27. Haberzett R, et al. Animal models of the serotonin syndrome: a systematic review. Behav Brain Res. 2013;256:328–45.
28. Chiew AL, Buckley NA. The serotonin toxidrome: shortfalls of current diagnostic criteria for related syndromes. Clin Toxicol (Phila). 2022;60:143.
29. FDA. Guidance for Industry: Q1A(R2) Stability testing of new drug substances and products, U.S. Department of Health and Human Services, Food and Drug Administration. Substance. 2003;1–22
30. Jurišić Dukovski B, Mrak L, Winnicka K, Szekalska M, Juretić M, Filipović-Grčić J, et al. Spray-dried nanoparticle-loaded pectin microspheres for dexamethasone nasal delivery. Dry Technol [Internet]. Taylor & Francis; 2019;37:1915–25. Available from: https://doi.org/10.1080/07373937.2018.1545783
31. Khair R, Shende P, Kulkarni YA. Nanostructured polymer-based cochleates for effective transportation of insulin. J Mol Liq [Internet]. Elsevier B.V.; 2020;311:113352. Available from. https://doi.org/10.1016/j.molliq.2020.113352
32. Tahir N, Madni A, Balasubramanian V, et al. Development and optimization of methotrexate-loaded lipid-polymer hybrid nanoparticles for controlled drug delivery applications. Int J Pharm. 2017;533(1):156–68. https://doi.org/10.1016/j.ijpharm.2017.09.061.
33. Schubert MA, Schicke BC, Müller-Goymann CC. Thermal analysis of the crystallization and melting behavior of lipid matrices and lipid nanoparticles containing high amounts of lecithin. Int J Pharm. 2005;298:242–54.
34. Mahmood S, Kiong KC, Tham CS, Chien TC, Hilles AR, Venugopal JR. PEGylated lipid polymeric nanoparticle-encapsulated acyclovir for in vitro controlled release and ex vivo gut sac permeation. AAPS PharmSciTech. 2020;21(7):285. https://doi.org/10.1208/s12249-020-01810-0.
35. Bonechi C, Martini S, Ciani L, et al. Using liposomes as carriers for polyphenolic compounds: the case of trans-resveratrol. PLoS ONE. 2012;7(8):e41438. https://doi.org/10.1371/journal.pone.0041438.
36. Mohammad HA, Ghareeb MM, Akrami M, Sahib AS. Design and characterization of Tacrolimus monohydrate loaded core shell lipid polymer hybrid nanoparticle. J Complement Med Res. 2020;11(5):204–14.
37. Mandal B, Bhattacharjee H, Mittal N, Sah H, Balabathula P, Thoma LA, Wood GC. Core-shell-type lipid-polymer hybrid nanoparticles as a drug delivery platform. Nanomed Nanotechnol Biol Med. 2013;9(4):474–91. https://doi.org/10.1016/j.nano.2012.11.010.
38. Nguyen TTL, Maeng HJ. Pharmacokinetics and pharmacodynamics of intranasal solid lipid nanoparticles and nanostructured lipid carriers for nose-to-brain delivery. Pharmaceutics. 2022;14.
39. Garg NK, Tandel N, Bhadada SK, Tyagi RK. Nanostructured lipid carrier–mediated transdermal delivery of aceclofenac hydrogel present an effective therapeutic approach for inflammatory diseases. Front Pharmacol. 2021;12:1–18.
40. Bekhti F, Mokhtari-Soulimane N, Bensalah M, Wacila N, Badi Z, Rouigueb K, Tewfik S, Tofail SAM, Helen T, Nanasaheb T. Histological injury to rat brain, liver, and kidneys by gold nanoparticles is dose-dependent. ACS Omega. 2022;7(24):20656–65. https://doi.org/10.1021/acsomega.2c00727.
41. Isbister GK, Buckley NA. The pathophysiology of serotonin toxicity in animals and humans. Clin Neuropharmacol. 2005;28(5):205–14. https://doi.org/10.1097/01.wnf.0000177642.89888.85.
42. Mohammad A, Ghareeb M. Tacrolimus monohydrate loaded lipid polymer hybrid nanoparticles Formulation and stability study. Kerbala J Pharm Sci. 2021;1(19).
43. Bershteyn A, Chaparro J, Yau R, Kim M, Reinherz E, Ferreira-Moita L, et al. Polymer-supported lipid shells, onions, and flowers. Soft Matter. 2008;4:1787–91.
44. Galgatte UC, Kumbhar AB, Chaudhari PD. Development of in situ gel for nasal delivery: design, optimization, in vitro and in vivo evaluation. Drug Deliv. 2014;21(1):62–73. https://doi.org/10.3109/10717544.2013.849778.
45. Ma Z, Zhang G, Jenney C, Krishnamoorthy S, Tao R. Characterization of serotonin-toxicity syndrome (toxidrome) elicited by 5-hydroxy-l-tryptophan in clorgyline-pretreated rats. Eur J Pharmacol. 2008;588:198–206.